Dinucleating Hybrid Ligands Providing a "Soft" P∩N and an Adjacent N-Rich Coordination Pocket − Controlled Synthesis of Unsymmetric Homodinuclear and Heterodinuclear Complexes

Matthias Konrad,[a] Susanne Wuthe,[a] Franc Meyer,*[a] and Elisabeth Kaifer[a]

Dedicated to Prof. Dr. Ernst-G. Jäger on the occasion of his 65th birthday

Keywords: Bridging ligands / Nickel / P,N ligands / Palladium / Bimetallic complexes

New unsymmetric dinucleating pyrazolate ligands with different chelating side arms in the 3- and 5-positions of the heterocycle have been prepared. These ligands provide a "soft" P∩N site and either an adjacent "N_3" (HL^a) or "N_2S_2" (HL^b) coordination pocket, and they have been employed to build homo- and heterobimetallic complexes featuring various types of asymmetry. Both L^a and L^b form the mixed-spin dinickel(II) chloride systems **4** and **5**, respectively, which in the former case dimerizes via Cl bridges to give a tetranuclear compound. In the heterobimetallic complex **6** the Pd^{II} is specifically housed within the P∩N compartment. All new complexes have been characterized by X-ray crystallography, and conformational and electronic coupling between the two metal ions of the dinuclear scaffolds have been analyzed.

Introduction

At present, research on di- and oligonuclear transition metal complexes is a flourishing field with major interests focused on the modeling of metallobiosites and on cooperative phenomena in catalysis and magnetism.[1−4] Among the diverse ligand frameworks designed and employed to hold two metal centers in close proximity and to induce the sought-after cooperativity, pyrazole derivatives appear particularly suited due to their well-known ability to span adjacent metal ions at a favorable distance.[5] Further control of the metal−metal separation, as well as of the steric and electronic properties of the individual metal ions can be achieved by appropriate chelating side arms attached to the 3- and 5-positions of the heterocycle. Most of these multidentate pyrazolate systems known to date are of the symmetric type,[6−11] although the individual metal ions are often assumed to play quite distinct roles in bimetallic catalysis, both in nature and in synthetic systems. The development of unsymmetrical dinucleating ligands that would give unsymmetric homobimetallic complexes, or might allow the controlled synthesis of heterobimetallic complexes is thus highly desirable.[2] However, a major obstacle to a more widespread use of such systems is their limited accessibility since, in general, the synthesis of unsymmetrical dinucleating ligands is much more arduous than the synthesis of the symmetrical analogues. Recently, we developed a versatile synthetic route which provides access to asymmetric pyrazole-based ligand matrices, providing two different coordination compartments.[11] These ligands enabled a predictable preparation of bimetallic complexes that exhibit various kinds of asymmetry. Initial emphasis was laid on the design and study of dinucleating systems that provide chemically distinct N- and S-rich donor atom sets for the two metal ions. Following the same synthetic strategy, we now report on the preparation and coordination chemistry of new compartmental type **A** ligands (Scheme 1) that comprise a bidentate P∩N binding site and an adjacent N-rich coordination pocket. Chelating P∩N ligands have been extensively used in organometallic chemistry, in particular in palladium-catalyzed reactions.[12] It is our intention in this context to tune the activity or selectivity of substrate transformations occurring at such organometallic centers by the cooperative effect of a second Lewis acidic metal ion positioned in close proximity of the active site. The present contribution lays a foundation for this goal by providing appropriate ligand frameworks that might help to preorganize the two metal ions, and by demonstrating the suitability of these new ligands for the building of heterobimetallic Pd−M complexes.

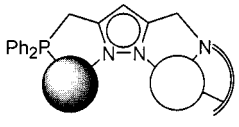

A

Scheme 1

Results and Discussion

Ligand Synthesis

The synthesis of type **A** ligands was accomplished according to the strategy developed previously (Scheme 2).[11] The unsymmetrically substituted pyrazole derivative **1** is

[a] Anorganisch-Chemisches Institut der Universität Heidelberg, Im Neuenheimer Feld 270, 69120 Heidelberg, Germany
Fax: (internat.) + 49-(0)6221/545707
E-mail: franc.meyer@urz.uni-heidelberg.de

  1434−1948/01/0909−2233 $ 17.50+.50/0

obtained by cycloaddition of ethyl diazoacetate and propynol,[13] and subsequent treatment with thionyl chloride.[11] Of the two different side arms, the diphenylphosphanyl moiety is introduced first by treating **1** with $KPPh_2$ to establish the P∩N site. The ester group in **2** is then converted into an amide function by treatment with different lithiated amines. Reduction of the resulting amide in **3a**,**b** completes the assembly of the second coordination compartment, which provides an "N_3" donor set in HL^a or an "N_2S_2" donor set in HL^b. The complexation potential of such individual P∩N,[6] "N_3"[10] and "N_2S_2"[11] sites has previously been explored to some extent in coordination compounds of related symmetric pyrazolate ligand systems.

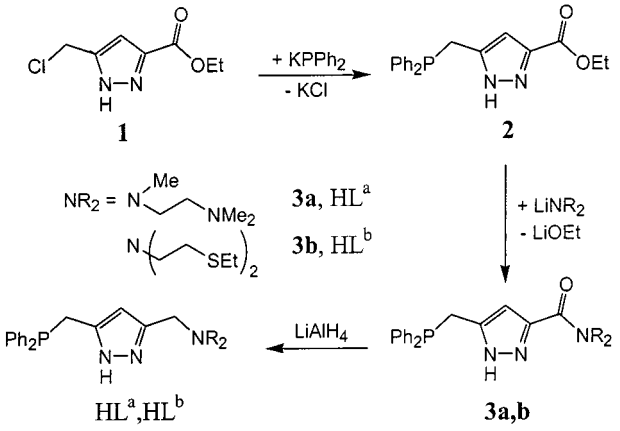

Scheme 2

Synthesis and Structural Characterization of Complexes

Homobimetallic dinickel(II) complexes of HL^a and HL^b were studied in order to provide some insight into the specific coordination behavior of the different donor sites.

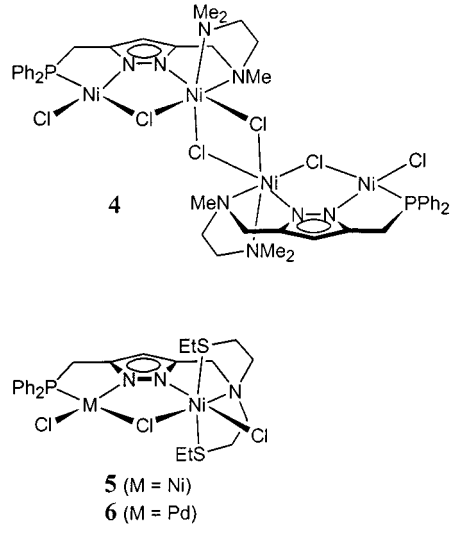

Scheme 3

Complexes $[L^aNi_2Cl_3]_2$ (**4**) and $L^bNi_2Cl_3$ (**5**) (Scheme3) were prepared by deprotonation of the pyrazole ligand with KO*t*Bu and subsequent treatment with 2 equiv. of $NiCl_2{\cdot}6H_2O$. Crystalline red material was obtained by diffusion of petroleum ether into solutions of the products in CH_2Cl_2 (**5**) or $CH_2Cl_2/CHCl_3$ (**4**), respectively. Complex **4** crystallizes in the space group *Pbcn*, while **5** crystallizes in the space group *Pc* with two independent molecules in the unit cell. The molecular structures of the complexes as determined by X-ray crystallography are depicted in Figures 1 and 2 together with selected atom distances and bond angles.

In both cases, the nickel ions are nested within their respective coordination compartments. The P∩N donor set exerts a stronger ligand field and brings about a low-spin configuration with an approximate square-planar coordination environment around its bound nickel ion [sum of the four angles around Ni1 in **4** 360.3(7)° and around Ni2 in **5** 359.9(6)°; magnetic measurements confirm the presence of only one high-spin nickel(II) ion per bimetallic entity in both **4** and **5**]. In contrast, the nickel ions in the "N_3" and "N_2S_2" sites are six-coordinate, which in the former case results from dimerization of two pyrazolate-based bimetallic moieties through a double Cl bridge to form the tetranuclear compound $[L^aNi_2Cl_3]_2$ (**4**). Similar structural motifs have also been observed for nickel chloride complexes of related symmetric pyrazolate ligand systems providing either two "N_3" or two "N_2S_2" compartments.[10,11] According to a common classification,[2a,14] **4** and **5** exhibit various kinds of asymmetry, e.g. donor atom asymmetry and coordination number asymmetry. As expected, bond lengths are generally shorter for the low-spin nickel(II) ions, which is most obvious for the asymmetrically bridging Cl2 atom within each pyrazolate-based dinuclear array: d(Ni1−Cl2) = 2.240(9) Å versus d(Ni2−Cl2) = 2.512(1) Å in **4** and d(Ni2−Cl2) = 2.255(2)/2.275(1) Å versus d(Ni1−Cl2) = 2.436(4)/2.432(8) Å in **5**. The double Cl bridges in **4** are asymmetric as well: d(Ni2−Cl3) = 2.394(5) versus d(Ni2−Cl3 A) = 2.456(7) Å. In all cases the distance between the low-spin Ni^{II} and the Cl atom *trans* to P is significantly larger than those between the low-spin Ni^{II} and the terminal Cl, because of the greater *trans* influence of the P ligand and the bridging position of the former Cl atom. A number of rather short interactions (< 3.0 Å) with C−H groups are present for all Cl ligands, which may be considered as weak hydrogen-bond interactions.[15]

Owing to the very different characteristics of their adjacent donor compartments, HL^a and HL^b appear to be well preorganized for the controlled synthesis of bimetallic complexes containing two different metal ions in distinct environments. When HL^b was first deprotonated and subsequently treated with 1 equiv. each of $PdCl_2$ and $NiCl_2{\cdot}6H_2O$ in a sequential fashion, the heterobimetallic green complex $L^bNiPdCl_3$ (**6**) was obtained in excellent yield. FAB mass spectrometry did confirm the heterodinuclear nature of the complex and did not reveal any indication of the presence of its homobimetallic analogues, i.e. of **5** or $L^bPd_2Cl_3$, thus suggesting that the complexation reaction is highly selective and that each of the different metal ions binds specifically to one of the distinct ligand compartments.

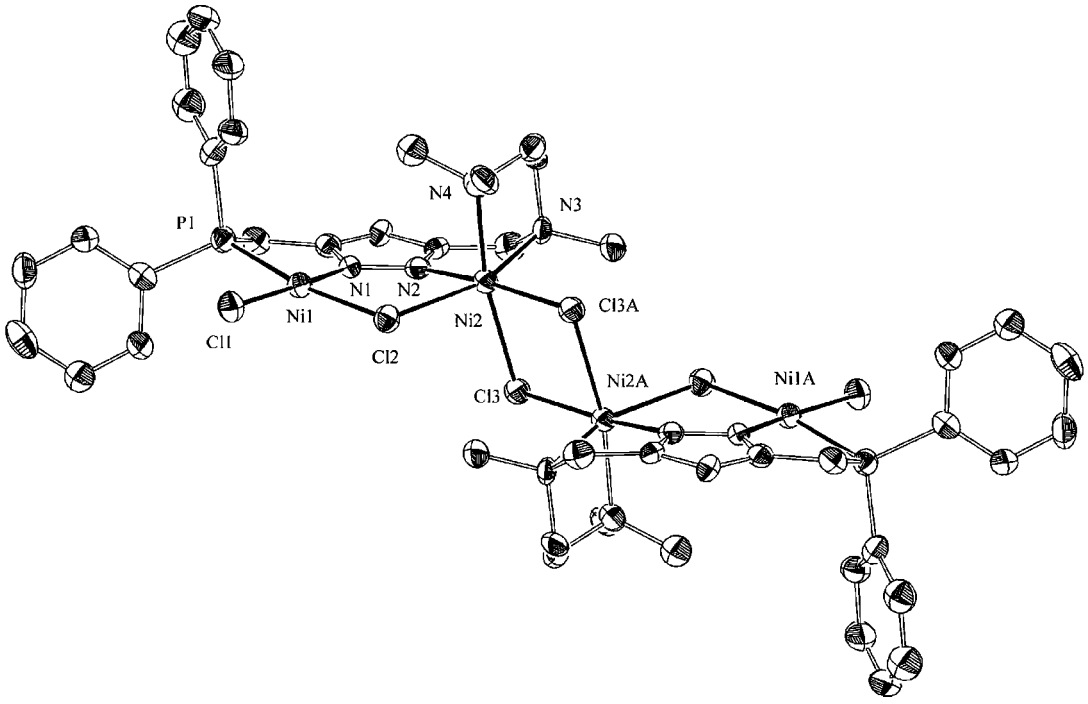

Figure 1. View of the molecular structure of **4**; in the interests of clarity all hydrogen atoms have been omitted; selected interatomic distances [Å] and bond angles [°]: Ni1−N1 1.869(2), Ni1−P1 2.155(8), Ni1−Cl1 2.171(6), Ni1−Cl2 2.240(9), Ni2−N2 1.997(2), Ni2−N3 2.200(3), Ni2−N4 2.151(2), Ni2−Cl2 2.512(3), Ni2−Cl3 2.394(5), Ni2−Cl3A 2.456(7), Ni1···Ni2 3.780(6), Ni2···Ni2A 3.705(1); Ni1−Cl2−Ni2 105.24(3), Ni2−Cl3−Ni2A 99.58(3), N1−Ni1−P1 83.06(7), P1−Ni1−Cl1 91.75(3), Cl1−Ni1−Cl2 92.76(3), Cl2−Ni1−N1 92.80(7)

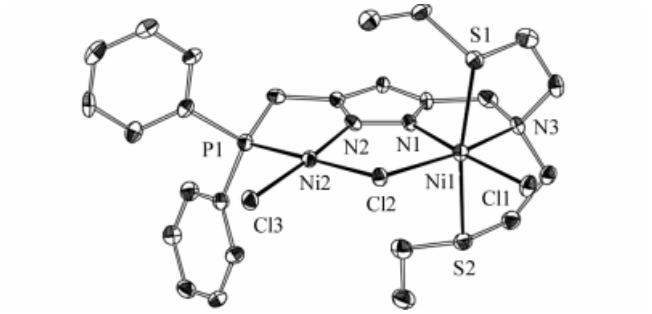

Figure 2. View of the structure of one of the two independent molecules of **5**; in the interests of clarity all hydrogen atoms have been omitted; selected interatomic distances [Å] and bond angles [°] [values for the second independent molecule in brackets]: Ni1−N1 1.958(5) [1.989(5)], Ni1−N3 2.151(5) [2.168(5)], Ni1−Cl1 2.357(2) [2.384(1)], Ni1−Cl2 2.436(4) [2.432(8)], Ni1−S1 2.473(2) [2.428(1)], Ni1−S2 2.435(1) [2.439(1)], Ni2−N2 1.857(5) [1.855(5)], Ni2−P1 2.137(2) [2.141(2)], Ni2−Cl2 2.255(2) [2.275(1)], Ni2−Cl3 2.168(1) [2.158(2)], Ni1···Ni2 3.697(5) [3.707(2)]; Ni1−Cl2−Ni2 103.9(5) [103.8(4)], N2−Ni2−P1 84.4(5) [83.6(8)], P1−Ni2−Cl3 88.6(4) [88.5(1)], Cl3−Ni2−Cl2 93.4(1) [94.4(1)], Cl2−Ni2−N2 93.4(8) [93.3(2)]

Two different types of single crystals suitable for a crystallographic analysis were obtained by layering solutions of complex **6** in CH_2Cl_2 with light petroleum ether. In one form (**6′**), the compound crystallizes in the space group *Pn* with two independent molecules in the unit cell. In the second form (**6′′**), the compound crystallizes in the space group $P2_1/n$ with two CH_2Cl_2 solvent molecules included in the crystal lattice. The overall constitution of **6** is the same in both crystal forms, but details of its molecular features are distinct, as described below. The structures of **6′′** and of one of the two independent (but similar) molecules of **6′** are depicted in Figures 3a and b together with selected atom distances and bond angles.

The bimetallic framework of **6** is closely related to the structure of its homobimetallic dinickel(II) analogue **5**. As anticipated, the palladium atom is found in an approximate square-planar environment within the P∩N pocket, while the nickel ion is located in the "N_2S_2" compartment. Geometric parameters of the Pd fragment are as expected [sum of the four angles around the Pd atom equal to 359.9(6)/360.0(6)/359.9(2)° for **6′** and **6′′**, respectively] and are comparable with the findings for a related $PdCl_2$ complex of a mononucleating pyrazolate-based P∩N ligand.[16] Geometric characteristics of the nickel ions housed in the "N_2S_2" compartments are basically identical for all cases. In particular, the Ni1("N_2S_2")−N1(pyrazole) bond lengths are found in the same range [1.965(5) − 1.991(5) Å] for **5**, **6** and for the symmetric ("N_2S_2")$_2$ complex reported previously.[11] This suggests that the choice of the second metal ion (high-spin Ni^{II} or low-spin Ni^{II}, or Pd^{II}) may only have a slight influence on the electronic properties of the six-coordinate nickel ion within the "N_2S_2" binding pocket. This is further analyzed by means of electrochemical experiments as described below.

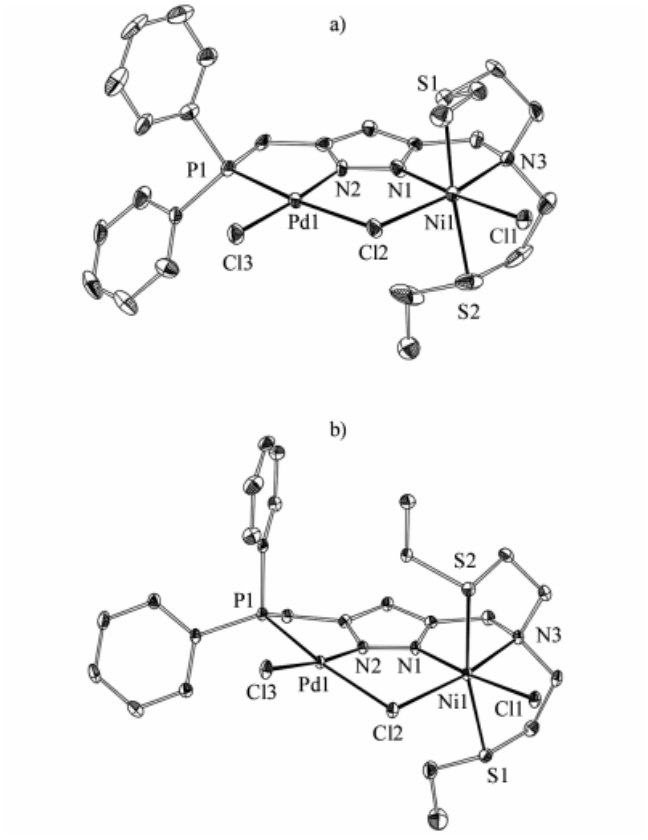

Figure 3. View of the structures of **6′** (a) (one of the two independent molecules) and **6′′** (b); in the interests of clarity all hydrogen atoms have been omitted; selected interatomic distances [Å] and bond angles [°]: **6′** [values for the second independent molecule in brackets]: Pd1−N2 1.989(7) [2.010(7)], Pd1−P1 2.219(2) [2.214(3)], Pd1−Cl2 2.395(2) [2.394(2)], Pd1−Cl3 2.299(2) [2.296(2)], Ni1−N1 1.981(6) [1.986(8)], Ni1−N3 2.166(7) [2.171(7)], Ni1−S1 2.455(2) [2.454(3)], Ni1−S2 2.397(3) [2.464(3)], Ni1−Cl1 2.366(2) [2.325(3)], Ni1−Cl2 2.452(2) [2.420(2)], Pd1···Ni1 3.808(2) [3.779(2)]; Pd1−Cl2−Ni1 103.57(8) [103.44(9)], N2−Pd1−P1 81.6(2) [81.7(2)], P1−Pd1−Cl3 94.11(8) [93.50(9)], Cl3−Pd1−Cl2 91.98(8) [93.21(9)], Cl2−Pd1−N2 92.3(2) [91.5(2)]; **6′′**: Pd1−N2 1.993(2), Pd1−P1 2.221(1), Pd1−Cl2 2.425(5), Pd1−Cl3 2.313(7), Ni1−N1 1.984(2), Ni1−N3 2.173(2), Ni1−S1 2.408(5), Ni1−S2 2.427(1), Ni1−Cl1 2.369(3), Ni1−Cl2 2.479(2), Pd1···Ni1 3.806(4); Pd1−Cl2−Ni1 101.79(3), N2−Pd1−P1 81.84(7), P1−Pd1−Cl3 92.54(3), Cl3−Pd1−Cl2 96.00(3), Cl2−Pd1−N2 89.49(7)

The most noticeable difference between the various crystalline forms of **6** is the conformation adopted by the five-membered chelate ring of the bidentate P∩N site and the resulting displacement of the P and Pd atoms out of the plane defined by the pyrazolate heterocycle. This is best visualized from a superposition of the P∩N subunits of the individual solid-state molecular structures of **6** shown in Figure 4 (one of the two independent molecules of **5** has been included as well, although the metal−ligand bond lengths are slightly shorter for Ni than for Pd). These various structures reflect individual geometric points on the pathway of interconversion between the λ and the δ conformers of the five-membered chelate ring. A trajectory of such fluxional motion has to pass through a flattened planar ring structure, which is represented by one of the two independent molecules of **6′** (see also Figure 3a). The observation of different static geometries for the P∩N chelate ring located between the limiting λ and δ conformers − which at the same time exhibit very similar geometric arrangements of the Ni("N_2S_2") coordination site − confirms that the two subunits of the bimetallic pyrazolate framework are conformationally largely decoupled. Conformational interconversion of the P∩N coordination unit is evidently facile, and each particular situation observed in the solid state should thus be mainly determined by intermolecular crystal-packing interactions.

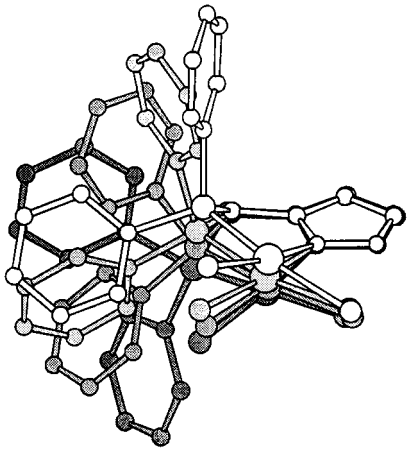

Figure 4. Overlay of the P∩N fragments of the solid-state structures of **5** (one of the two independent molecules), **6′** (both independent molecules), and **6′′**

Spectroscopy and Electrochemistry

While any comprehensive NMR-spectroscopical characterization of the complexes is hampered by their paramagnetic nature, broad low-field shifted ^{31}P NMR signals of the diamagnetic subunits are still found at δ = +241 and +257 for CD_2Cl_2 solutions of **4** and **5**, respectively. In the case of **6**, poor solubility precludes the detection of its ^{31}P NMR resonance.

The electronic absorption spectrum of **6** in CH_2Cl_2/MeCN (5:1) shows two weak bands at λ = 1100 (ν_1; ε = 26 $M^{-1}\cdot cm^{-1}$) and 620 nm (ν_2; ε = 12 $M^{-1}\cdot cm^{-1}$) that are assigned to spin-allowed transitions from $^3A_{2g}$ to $^3T_{2g}$ and $^3T_{1g}(F)$ for the six-coordinate Ni^{II}. The ν_3 band [$^3A_{2g}$ to $^3T_{1g}(P)$] expected for a near-octahedral d^8 ion[17] seems to be masked by strong high-energy absorptions extending as low as λ = 450 nm [peaks at λ = 336 nm (ε = 1710 $M^{-1}\cdot cm^{-1}$) and 301 nm (ε = 2620 $M^{-1}\cdot cm^{-1}$)]. These bands presumably correspond to intraligand and LMCT excitations. From the ν_1 band a ligand-field value of Δ_{oct} = 9090 cm^{-1} can be deduced for the nickel(II) ion in **6**. Complex **5** likewise features a low-intensity ν_1 band (λ = 1095 cm^{-1}; ε = 35 $M^{-1}\cdot cm^{-1}$), indicating Δ_{oct} = 9130 cm^{-1}. The almost identical ligand-field splitting observed for the high-spin Ni^{II} in both **5** and **6** confirms the conclusion already derived from the structural data, i.e. the choice of the second metal ion (either Pd^{II} in **6** or low-spin Ni^{II} in **5**) does not significantly alter the electronic situation at the high-spin ("N_2S_2")Ni^{II} site. Δ_{oct} for a related symmetrical dinickel(II)

complex that is composed of two identical "N_2S_2" compartments was found to be 8730 cm^{-1}.[11] An additional strong absorption for **5** at $\lambda = 498$ nm ($\varepsilon = 690$ $M^{-1}\cdot cm^{-1}$) is assigned to the square-planar low-spin Ni^{II}, presumably masking the much weaker ν_2 band. Intraligand and LMCT excitations dominate the spectrum of **5** below 350 nm, but a further d-d absorption is discernible as a shoulder at $\lambda =$ 379 nm ($\varepsilon \approx 645$ $M^{-1}\cdot cm^{-1}$).

Complexes **5** and **6** have been studied by cyclic voltammetry in CH_2Cl_2 solution (Figure 5). The dinickel(II) complex **5** undergoes a quasi-reversible oxidation at +1.00 V ($\Delta E = 162$ mV) versus the saturated calomel electrode (SCE), closely followed by further anodic processes at higher potential. The first oxidation wave at +1.00 V can be assigned to the six-coordinate nickel ion within the "N_2S_2" compartment, by comparison with the electrochemical properties of the PdNi compound **6** as well as the symmetric ("N_2S_2")$_2$dinickel(II) complex studied previously.[11] Complex **6** features a reversible oxidation at $E_{1/2} = +1.04$ V [i_{pa}/i_{pc} close to 1; $i_{pc}/v^1/_2 \approx$ const.; $\Delta E_p = 115$ mV with $\Delta E_p(Cp_2Fe/Cp_2Fe^+) = 120$ mV under the same experimental conditions] that is assigned to the formation of the $Pd^{II}Ni^{III}$ species. In this case, further oxidation processes are only observed at much higher potentials above +1.5 V. Obviously, oxidation of the nickel ion in the "N_2S_2" binding pocket is not significantly influenced by the choice of either a low-spin Ni^{II} or a Pd^{II} ion in the nearby P∩N site. This is in accordance with the above interpretation of the electronic spectra and structural features of **5** and **6**. The symmetric ("N_2S_2")$_2$dinickel(II) complex was shown to undergo a reversible first oxidation at $E_{1/2} = +0.87$ V, followed by a further oxidation process at $E_p^{ox} = +1.26$ V, indicating that Ni^{III} within the "N_2S_2" compartment is somewhat more efficiently stabilized by a second high-spin Ni^{II} ion than by an adjacent low-spin Ni^{II} (or Pd^{II}) as in **5** and **6**. Cathodic processes are irreversible for both **5** and **6**, with $E_p^{red} = -1.22$ V for the NiNi compound, and an ill-defined cyclic voltammetric response with a peak around −1.6 V for the PdNi species (all values at scan rate 200 mVs^{-1}).

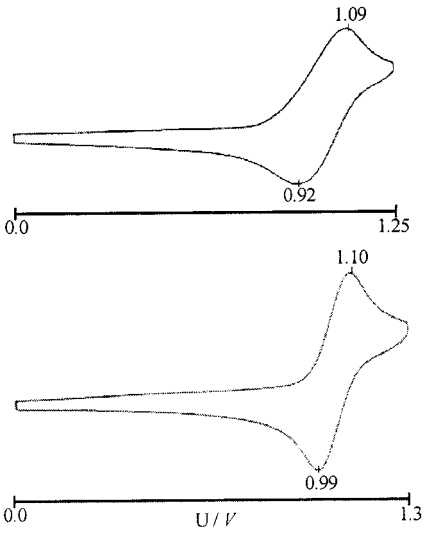

Figure 5. Cyclic voltammograms of complex **5** (top) and **6** (bottom) in CH_2Cl_2 containing 0.1 M $nBu_4N^+PF_6^-$ at a scan rate of 200 mVs^{-1}

Conclusions

New dinucleating ligands have been synthesized that feature two distinct binding pockets: a "soft" P∩N site, and either an adjacent "N_3" (HL^a) or "N_2S_2" (HL^b) compartment. These systems proved suitable for the preparation of unsymmetric bimetallic complexes in a controlled and predetermined fashion. In homobimetallic $(Ni^{II})_2$ compounds, a mixed-spin configuration is enforced by the strongly different ligand fields of the two binding pockets, while in a heterobimetallic $Ni^{II}Pd^{II}$ complex the different metal ions are selectively incorporated into their respective binding pockets, i.e. the Pd^{II} is exclusively nested in the P∩N site. Structural, spectroscopic and electrochemical features of the bimetallic systems indicate that the two coordination subunits are only moderately coupled with regard to conformational and electronic aspects. It is now hoped that these ligands will provide tailored scaffolds for the synthesis of novel bimetallic systems combining an organometallic and a Werner-type fragment in close proximity, which might enable unusual cooperative effects in metal-mediated substrate transformations.

Experimental Section

General Procedures and Methods: All manipulations were carried out under dry nitrogen by employing standard Schlenk techniques. Compound **1** was prepared as reported.[11] Solvents were dried according to established procedures, all other chemicals were used as purchased. Microanalyses: Mikroanalytische Laboratorien des Organisch-Chemischen Instituts der Universität Heidelberg. − NMR spectra: Bruker AC 200 at 200.13 (^{1}H) and 50.32 (^{13}C) MHz; solvent signal as chemical shift reference ($CDCl_3$: $\delta_H = 7.27$; $\delta_C = 77.0$). − Cyclic voltammetry: PAR equipment (potentiostat/galvanostat 273), in 0.1 M Bu_4NPF_6/CH_2Cl_2. Potentials in V on glassy carbon electrode, referenced to SCE at ambient temperature. − IR spectra: Perkin−Elmer 983G; recorded as KBr pellets. − FAB-MS spectra: Finnigan MAT 8230. − UV/Vis spectra: Perkin−Elmer Lambda 19; recorded in CH_2Cl_2 (**5**) or CH_2Cl_2/MeCN 5:1 (**6**). − Magnetic measurement: Bruker Magnet B-E 15 C8, field-controller B-H 15, Sartorius microbalance M 25 D-S. Experimental susceptibility data were corrected for the underlying diamagnetism.

Ethyl 5-[(Diphenylphosphanyl)methyl]-1*H*-pyrazole-3-carboxylate (2): A solution of diphenylphosphane (4.1 g, 22.0 mmol) in THF (100 mL) was treated with 1 equiv. of KO*t*Bu (2.5 g, 22.0 mmol). The red solution was stirred for 1 h, cooled to −70 °C and a solution of ethyl 5-(chloromethyl)pyrazole-3-carboxylate[11] (1.9 g, 10.0 mmol) in THF (50 mL) was slowly added. After warming to room temperature, the solution was left stirring overnight, then quenched with saturated NH_4Cl solution. The organic phase was dried with $MgSO_4$ and filtered. The solvent was evaporated in vacuum and the residue was redissolved in a small amount of Et_2O. The product was precipitated as a white powder by addition of light petroleum ether, filtered and dried in vacuum to yield 2.9 g

(8.5 mmol, 85%) of **2**. – ^{1}H NMR: δ = 1.33 (t, J_{HH} = 7.1 Hz, 3 H, CH_3), 3.51 (s, 2 H, PCH_2), 4.31 (q, J_{HH} = 7.1 Hz, 2 H, OCH_2), 6.51 (s, 1 H, CH^{pz}), 7.30–7.45 (m, 10 H, CH^{ar}). – ^{13}C NMR: δ = 14.0 (CH_3), 25.8 (d, $^1J_{CP}$ = 15.9 Hz, PCH_2), 60.6 (OCH_2), 107.3 (d, $^3J_{CP}$ = 5.3 Hz, $C^{pz,4}$), 128.3–132.6 (C^{ar}), 137.2 (d, $^2J_{CP}$ = 14.6 Hz, $C^{q,ar}$), 140.8 ($C^{pz,3}$), 143.4 (d, $^1J_{CP}$ = 10.9 Hz, $C^{pz,5}$), 161.5 (CO). – ^{31}P NMR: δ = –16.4. – MS (FAB*): m/z* (%) = 338 (100) [M^+], 309 (10) [M^+ – Et], 292 (12) [M^+ – OEt], 261 (9) [M^+ – Ph], 185 (100) [PPh_2^+], 183 (95) [dibenzophosphole$^+$]. – $C_{19}H_{19}N_2O_2P$ (338.35): calcd. C 67.45, H 5.66, N 8.28; found C 66.71, H 5.70, N 8.15.

***N*-[2-(Dimethylamino)ethyl]-5-[(diphenylphosphanyl)methyl]-*N*-methyl-1*H*-pyrazole-3-carboxamide (3a):** A solution of BuLi (3.4 mL, 2.5 M) in hexane was added to a solution of trimethylethylenediamine (1.8 g, 17.2 mmol) in THF (75 mL) at –70 °C. This mixture was slowly added to a solution of **2** (2.9 g, 8.6 mmol) in THF (150 mL) at –70 °C. After warming to room temperature, the solution was left stirring overnight, then quenched with saturated NH_4Cl solution and the aqueous phase extracted several times with Et_2O. The combined organic phases were dried with $MgSO_4$ and filtered. After evaporation of the solvent in vacuum, the product **3a** (2.7 g, 81%) remained as a yellow oil. – ^{1}H NMR: δ = 2.30 (s, 6 H, NMe_2), 2.57 (m, 2 H, CH_2), 3.01/3.15 (br, 3 H, NMe, *Z*/*E*), 3.44 (s, 2 H, PCH_2), 3.57 (br, 2 H, CH_2), 6.15/6.33 (br, 1 H, CH^{pz}), 7.29–7.44 (m, 10 H, CH^{ar}). – ^{13}C NMR: δ = 27.2 (br, PCH_2), 33.8/37.1 (NMe, *Z*/*E*), 46.2 (NMe_2), 45.5/49.5 (CH_2, *Z*/*E*), 56.4/57.1 (CH_2, *Z*/*E*), 106.8/107.5 ($C^{pz,4}$), 128.4–132.8 (C^{ar}), 138.0 (d, $^1J_{CP}$ = 10.7 Hz, $C^{q,ar}$), $C^{pz,3}$/$C^{pz,5}$ not observed, 162.4 (CO). – ^{31}P NMR: δ = –16.5. – MS (EI): *m/z* (%) = 395 (16) [M^+], 58 (100) [$CH_2NMe_2^+$]. – $C_{22}H_{27}N_4OP$ (394.45): calcd. C 66.99, H 6.89, N 14.20, P 7.85; found C 66.98, H 7.05, N 13.80, P 8.24.

5-[(Diphenylphosphanyl)methyl]-*N*,*N*-bis[2-(ethylsulfanyl)ethyl]-1*H*-pyrazole-3-carboxamide (3b): Compound **3b** was synthesized as described for **3a** using bis[2-(ethylsulfanyl)ethyl]amine[11] (3.3 g, 17.2 mmol). Yield (3.8 g, 91%). – ^{1}H NMR: δ = 1.25 (m, 6 H, CH_3), 2.48–2.78 (m, 8 H, SCH_2), 3.46 (s, 2 H, PCH_2), 3.64 (m, br, 2 H, NCH_2), 3.79 (m, br, 2 H, NCH_2), 6.34 (s, 1 H, C^{pz}), 7.33–7.51 (m, 10 H, CH^{ar}). – ^{13}C NMR: δ = 14.7 (CH_3), 25.8/26.2 (PCH_2/SCH_2) 28.6/30.0 (SCH_2, *Z*/*E*), 47.6/49.4 (NCH_2, *Z*/*E*), 106.8 ($C^{pz,4}$), 128.3–132.6 (C^{ar}), 137.1 (d, $^1J_{CP}$ = 14.0 Hz, $C^{q,ar}$), $C^{pz,3}$/$C^{pz,5}$ not observed, 162.4 (CO). – ^{31}P NMR: δ= –17.0. – MS (EI): *m/z* (%) = 486 (8) [M^+], 457 (87) [M^+ – Et], 397 (54) [M^+ – CH_2CH_2SEt], 293 (68) [M^+ – $N(CH_2CH_2SEt)_2$], 185 (64) [PPh_2^+], 183 (76) [dibenzophosphole$^+$], 89 (100) [$CH_2CH_2SEt^+$]. – $C_{25}H_{32}N_3OPS_2$ (485.65): calcd. C 61.83, H 6.64, N 8.65; found C 61.68, H 6.63, N 8.02.

***N*²-{5-[(Diphenylphosphanyl)methyl]-1*H*-pyrazol-3-yl}-*N*¹,*N*¹,*N*²-trimethylethane-1,2-diamine (HL^a):** A solution of **3a** (2.7 g, 6.8 mmol) in THF (100 mL) was slowly added to a suspension of $LiAlH_4$ (0.24 g, 6.8 mmol) in THF (50 mL). After stirring overnight, the mixture was refluxed for 30 min, then cooled to 0 °C and hydrolyzed by dropwise addition of H_2O (0.5 mL), NaOH (0.5 mL, 15%) and H_2O (1.5 mL). The solids were filtered off and washed several times with Et_2O. The combined organic phases were dried with $MgSO_4$ and filtered. After evaporation of the solvent in vacuum, the product HL^a (2.1 g, 81%) remained as a colorless oil. – ^{1}H NMR: δ = 2.15 (s, 6 H, NMe_2), 2.18 (s, 3 H, NMe), 2.35 (m, 4 H, CH_2), 3.42 (s, 2 H, PCH_2), 3.48 (s, 2 H, NCH_2), 5.79 (s, 1 H, CH^{pz}), 7.25–7.43 (m, 10 H, CH^{ar}). – ^{13}C NMR: δ = 27.5 (br, PCH_2), 42.7 (NMe), 45.5 (NMe_2), 53.1 (br, CH_2), 54.2 (CH_2), 57.3 (CH_2), 103.9 (d, $^3J_{CP}$ = 5.1 Hz, $C^{pz,4}$), 127.8–132.9 (C^{ar}), 138.3 (d, $^1J_{CP}$ = 14.5 Hz, $C^{ar,q}$), $C^{pz,3}$/$C^{pz,5}$ not observed. – ^{31}P NMR: δ = –16.6. – MS (EI): *m/z* (%) = 380 (7) [M^+], 322 (44) [M^+ – CH_2NMe_2], 279 (40) [M^+ – $MeNCH_2CH_2NMe_2$], 185 (45) [PPh_2^+], 183 (80) [dibenzophosphole$^+$]. – $C_{22}H_{29}N_4P$ (380.47): calcd. C 69.45, H 7.68, N 14.73; found C 68.72, H 7.78, N 12.88.

***N*-{5-[(Diphenylphosphanyl)methyl]-1*H*-pyrazol-3-yl}-*N*,*N*-bis[(2-ethylsulfanyl)ethyl]amine (HL^b):** A solution of **3b** (3.8 g, 7.8 mmol) in THF (50 mL) was slowly added to a suspension of $LiAlH_4$ (0.27 g, 7.8 mmol) in Et_2O (100 mL). After stirring overnight, the mixture was refluxed for 30 min, then cooled to 0 °C and hydrolyzed by dropwise addition of H_2O (0.6 mL), NaOH (0.6 mL, 15%) and H_2O (1.8 mL). The solids were filtered and washed several times with Et_2O. The combined organic phases were dried with $MgSO_4$ and filtered. After evaporation of the solvent in vacuum, the product HL^b (2.2 g, 59%) remained as a colorless oil. – ^{1}H NMR: δ = 1.23 (t, J_{HH} = 7.3 Hz, 6 H, CH_3), 2.44–2.74 (m, 12 H, CH_2), 3.43 (s, 2 H, PCH_2), 3.64 (s, 2 H, NCH_2), 5.85 (s, 1 H, CH^{pz}), 7.33–7.49 (m, 10 H, CH^{ar}). – ^{13}C NMR: δ = 14.6 (CH_3), 25.9 (SCH_2), 27.3 (d, $^1J_{CP}$ = 14.8 Hz, PCH_2), 29.4 (SCH_2), 49.8 (NCH_2), 53.5 (NCH_2), 103.5 (d, $^3J_{CP}$ = 5.5 Hz, $C^{pz,4}$), 128.1–132.7 (C^{ar}), 138.0 (d, $^1J_{CP}$ = 14.3 Hz, $C^{ar,q}$), 143.7 (br, $C^{pz,3/5}$). – ^{31}P NMR: δ = –16.8. – IR (film): $\tilde{\nu}$ = 3180–2863 (vs), 1950/1870/1806 (w), 1565/1476 (s), 1446/1428 (vs), 1369/1302/1262/1182 (s), 1096 (vs), 1065/1024/997/803 (s), 741/695 cm^{-1} (vs). – MS (EI): *m/z* (%) = 471 (5) [M^+], 396 (100) [M^+ – CH_2SEt], 279 (78) [M^+ – $N(CH_2CH_2SEt)_2$], 185 (13) [PPh_2^+], 183 (16) [dibenzophosphole$^+$], 89 (61) [$CH_2CH_2SEt^+$]. – $C_{25}H_{34}N_3PS_2$ (471.67): calcd. C 63.66, H 7.27, N 8.91; found C 63.43, H 7.17, N 8.44.

($L^aNi_2Cl_3$)$_2$ (4): Solutions of KO*t*Bu (0.06 g, 0.5 mmol) in EtOH (30 mL) and $NiCl_2·6H_2O$ (0.37 g, 1.0 mmol) in EtOH (15 mL) were added stepwise to a solution of HL^a (0.19 g, 0.5 mmol) in THF (50 mL) at 0 °C. After stirring for 3 h, the solvent was evaporated in vacuum. Layering a solution of the product in CH_2Cl_2/$CHCl_3$ (1:1) with light petroleum ether afforded red crystals of **4** (0.24 g, 80%). – ^{31}P NMR: δ = 241 (br). – MS (EI): *m/z* (%) = 567 (100) [$L^aNi_2Cl_2^+$], 532 (31) [$L^aNi_2Cl^+$]. – $C_{44}H_{56}Cl_6N_8Ni_4P_2$ (1206.42): calcd. C 43.81, H 4.68, N 9.29; found C 44.32, H 5.38, N 8.62.

$L^bNi_2Cl_3$ (5): KO*t*Bu (0.06 g, 0.5 mmol) and a solution of $NiCl_2·6H_2O$ (0.37 g, 1.0 mmol) in EtOH (15 mL) were added stepwise to a solution of HL^b (0.24 g, 0.5 mmol) in CH_2Cl_2 (50 mL). The red reaction mixture was stirred for 3 h. After evaporation of the solvent, the remaining solid was washed with EtOH and Et_2O. Layering a solution of the product in CH_2Cl_2 with Et_2O afforded red crystals of **5** (0.28 g, 80%). – ^{31}P NMR (CD_2Cl_2): δ = 257 (br). – IR (KBr): $\tilde{\nu}$ = 2957–2861 (vs), 1461/1447 (w), 1430 (s), 1312/1255 (w), 1102 (s), 1062/1039/736/688/536 cm^{-1} (w). – MS (FAB): *m/z* (%) = 658 (70) [M^+ – Cl], 609 (100). – UV/Vis: λ (ε [$M^{-1}·cm^{-1}$]) = 379 (645, sh), 498 (690), 1095 nm (35). – M.p. > 240 °C. – $C_{25}H_{33}Cl_3N_3Ni_2PS_2$ (694.39): calcd. C 43.24, H 4.80, N 6.05; found C 42.75, H 4.70, N 5.93.

$L^bNiPdCl_3$ (6): KO*t*Bu (0.06 g, 0.5 mmol), $NiCl_2·6H_2O$ (0.12 g, 0.5 mmol) and $PdCl_2$ (0.09 g, 0.5 mmol) were added stepwise to a solution of HL^b (0.24 g, 0.5 mmol) in CH_2Cl_2 (50 mL). The product was isolated as described for **5** to yield green crystals of **6** (0.26 g, 69%). – IR (KBr): $\tilde{\nu}$ = 3084–2835 (vs), 1445 (w), 1429 (s), 1311/1256 (w), 1100 (s), 1065/1036/690/534 cm^{-1} (w). – MS (FAB): *m/z* (%) = 706 (100) [M^+ – Cl]. – UV/Vis: λ (ε [$M^{-1}·cm^{-1}$]) = 301 (2620), 336 (1710), 620 (12), 1100 nm (26). – $C_{25}H_{33}Cl_3N_3NiPPdS_2$ (741.12): calcd. C 40.52, H 4.49, N 5.67; found C 39.73, H 4.52, N 5.57.

X-ray Crystallography: The measurements were carried out with a Nonius–Kappa CCD diffractometer using graphite-monochrom-

Table 1. Crystal data and refinement details for complexes **4**, **5**, **6′** and **6′′**

	$[L^aNi_2Cl_3]_2$ (**4**)	$L^bNi_2Cl_3$ (**5**)	$L^bNiPdCl_3$ (**6′**)	$L^bNiPdCl_3$ (**6′′**)
Empirical formula	$C_{22}H_{28}Cl_3N_4Ni_2P{\cdot}CH_2Cl_2$	$C_{25}H_{33}Cl_3N_3Ni_2PS_2$	$C_{25}H_{33}Cl_3N_3NiPPdS_2$	$C_{25}H_{33}Cl_3N_3NiPPdS_2{\cdot}2CH_2Cl_2$
M_r	644.68	694.40	742.10	911.95
Crystal size [mm]	0.35 × 0.20 × 0.20	0.30 × 0.10 × 0.10	0.10 × 0.08 × 0.08	0.40 × 0.20 × 0.08
Crystal system	orthorhombic	monoclinic	monoclinic	monoclinic
Space group	*Pbcn*	*Pc*	*Pn*	$P2_1/n$
a [Å]	26.517(5)	14.162(3)	17.233(3)	12.754(3)
b [Å]	15.302(3)	13.263(3)	8.882(2)	15.913(3)
c [Å]	14.349(3)	15.756(3)	19.312(4)	18.178(4)
β [°]	90	98.75(3)	105.38(3)	104.26(3)
V [Å^3]	5822(2)	2925(1)	2850(1)	3576(1)
$\rho_{calcd.}$ [g cm^{-3}]	1.471	1.577	1.724	1.694
Z	8	4	4	4
T [K]	200	200	200	200
μ (Mo-K_α) [mm^{-1}]	1.734	1.780	1.797	1.739
Scan mode	ω	ω	ω	ω
hkl range	±34, ±19, ±17	±16, ±16, −19 to 17	±21, ±10, ±23	±16, −20 to 15, ±23
2θ range [°]	4.2−55.0	4.0−52.2	3.7−52.0	3.4−54.8
Measured refl.	12709	34726	11867	15240
Unique refl. (R_{int})	6576 (0.036)	11259 (0.105)	9972 (0.038)	8126 (0.032)
Observed refl. $I > 2\sigma(I)$	4871	4922	7777	6285
Refined parameters	314	608	608	388
Residual electron density [eÅ^{-3}]	0.77/−0.52	0.67/−0.50	1.10/−0.78	1.06/−1.04
R1	0.037	0.041	0.061	0.036
wR2 (all data)	0.097	0.065	0.101	0.075
Goodness-of-fit	1.041	0.621	1.048	1.020

ated Mo-K_α radiation. All calculations were performed using the SHELXT PLUS software package. Structures were solved by direct methods with the SHELXS-97 and refined with the SHELXL-97 program.[18] Atomic coordinates and thermal parameters of the non-hydrogen atoms were refined in anisotropic models by full-matrix least-squares calculation based on F^2. In general the hydrogen atoms were placed at calculated positions and allowed to ride on the atoms they are attached to. Table 1 compiles the data for the structure determinations. Crystallographic data (excluding structure factors) for the structures reported in this paper have been deposited with the Cambridge Crystallographic Data Centre as supplementary publication no. CCDC-159461 (**6′**), -159462 (**5**), -159463 (**6′′**) and -159464 (**4**). Copies of the data can be obtained free of charge on application to CCDC, 12 Union Road, Cambridge CB2 1EZ, UK [Fax: (internat.) + 44-1223/336-033; E-mail: deposit@ccdc.cam.ac.uk].

Acknowledgments

We are grateful to Prof. Dr. G. Huttner for his generosity and his continuous interest in our work. The Deutsche Forschungsgemeinschaft is sincerely thanked for a Heisenberg-fellowship (to F. M.) and the Fonds der Chemischen Industrie for financial support. A donation of $PdCl_2$ by Degussa AG (Hanau) is gratefully acknowledged.

[1] [1a] S. R. Collinson, D. E. Fenton, *Coord. Chem. Rev.* **1996**, *148*, 19−40. − [1b] H. Okawa, H. Sakiyama, *Pure Appl. Chem.* **1995**, *67*, 273−280. − [1c] L. Que, jun., Y. Dong, *Acc. Chem. Res.* **1996**, *29*, 190−196. − [1d] H. Steinhagen, G. Helmchen, *Angew. Chem.* **1996**, *108*, 2489−2492; *Angew. Chem. Int. Ed. Engl.* **1996**, *35*, 2339.

[2] [2a] D. E. Fenton, H. Okawa, *Chem. Ber./Recueil* **1997**, *130*, 433−442. − [2b] H. Okawa, H. Furutachi, D. E. Fenton, *Coord. Chem. Rev.* **1998**, *174*, 51−75.

[3] [3a] D. G. McCollum, B. Bosnich, *Inorg. Chim. Acta* **1998**, *270*, 13−19. − [3b] M. Shibasaki, H. Sasai, T. Arai, T. Iida, *Pure Appl. Chem.* **1998**, *70*, 1027−1034. − [3c] E. K. van den Beuken, B. L. Feringa, *Tetrahedron* **1998**, *54*, 12985−13011.

[4] [4a] O. Kahn, *Angew. Chem.* **1985**, *97*, 837−853. − [4b] O. Kahn, *Adv. Inorg. Chem.* **1995**, *43*, 179−259.

[5] [5a] S. Trofimenko, *Progr. Inorg. Chem.* **1986**, *34*, 115−210. − [5b] A. P. Sadimenko, S. S. Basson, *Coord. Chem. Rev.* **1996**, *147*, 247−297. − [5c] G. La Monica, G. A. Ardizzoia, *Progr. Inorg. Chem.* **1997**, *46*, 151−238. − [5d] L. A. Oro, M. A. Ciriano, C. Tejel, *Pure Appl. Chem.* **1998**, *70*, 779−788.

[6] [6a] T. G. Schenck, J. M. Downes, C. R. C. Milne, P. B. Mackenzie, H. Boucher, J. Whelan, B. Bosnich, *Inorg. Chem.* **1985**, *24*, 2334−2337. − [6b] [a] T. G. Schenck, C. R. C. Milne, J. F. Sawyer, B. Bosnich, *Inorg. Chem.* **1985**, *24*, 2338−2344.

[7] [7a] J. Casabó, J. Pons, K. S. Siddiqi, F. Teixidor, E. Molins, C. Miravitlles, *J. Chem. Soc., Dalton Trans.* **1989**, 1401−1403. − [7b] T. Kamiusuki, H. Okawa, E. Kitaura, M. Koikawa, N. Matsumoto, S. Kida, H. Oshio, *J. Chem. Soc., Dalton Trans.* **1989**, 2077−2081. − [7c] T. Kamiusuki, H. Okawa, N. Matsumoto, S. Kida, *J. Chem. Soc., Dalton Trans.* **1990**, 195−198. − [7d] J. Pons, X. López, E. Benet, J. Casabó, F. Teixidor, F. J. Sánchez, *Polyhedron* **1990**, *9*, 2839−2845. − [7e] T. Kamiusuki, H. Okawa, E. Kitaura, K. Inoue, S. Kida, *Inorg. Chim. Acta* **1991**, *179*, 139−143. − [7f] J. C. Bayón, P. Esteban, G. Net, P. G. Rasmussen, K. N. Baker, C. W. Hahn, M. M. Gumz, *Inorg. Chem.* **1991**, *30*, 2572−2574. − [7g] K. Shindo, Y. Mori, K. Motoda, H. Sakiyama, N. Matsumoto, H. Okawa, *Inorg. Chem.* **1992**, *31* 4987−4990. − [7h] C. Acerete, J. M. Bueno, L. Campayo, P. Navarro, M. I. Rodriguez-Franco, A. Samat, *Tetrahedron* **1994**, *50*, 4765−4774. − [7i] M. Itoh, K. Motoda, K. Shindo, T. Kamiusuki, H. Sakiyama, N. Matsumoto, H. Okawa, *J. Chem. Soc., Dalton Trans.* **1995**, 3635−3641. − [7j] S. Baitalik, U. Flörke, K. Nag, *Inorg. Chem.* **1999**, *38*, 3296−3308.

[8] [8a] L. Behle, M. Neuburger, M. Zehnder, T. A. Kaden, *Helv. Chim. Acta* **1995**, *78*, 693−702. − [8b] H. Weller, L. Siegfried, M. Neuburger, M. Zehnder, T. A. Kaden, *Helv. Chim. Acta* **1997**, *80*, 2315−2328.

[9] [9a] F. Meyer, S. Beyreuther, K. Heinze, L. Zsolnai, *Chem.*

Ber./Recueil **1997**, *130*, 605−613. − [9b] F. Meyer, A. Jacobi, L. Zsolnai, *Chem. Ber., Recueil* **1997**, *130*, 1441−1447. − [9c] F. Meyer, K. Heinze, B. Nuber, L. Zsolnai, *J. Chem. Soc., Dalton Trans.* **1998**, 207−213.

[10] F. Meyer, U. Ruschewitz, P. Schober, B. Antelmann, L. Zsolnai, *J. Chem. Soc., Dalton Trans.* **1998**, 1181−1186.

[11] M. Konrad, F. Meyer, K. Heinze, L. Zsolnai, *J. Chem. Soc., Dalton Trans.* **1998**, 199−205.

[12] See for example: [12a] P. von Matt, A. Pfaltz, *Angew. Chem.* **1993**, *105*, 614−615; *Angew. Chem. Int. Ed. Engl.* **1993**, *32*, 556−568. − [12b] A. Togni, U. Burckhardt, V. Gramlich, P. S. Pregosin, R. Salzmann, *J. Am. Chem. Soc.* **1996**, *118*, 1031−1037. − [12c] M. Sperrle, G. Consiglio, *Chem. Ber./Recueil* **1997**, *130*, 1557−1565. − [12d] G. Helmchen, *J. Organomet. Chem.* **1999**, *576*, 203−214. − [12e] K. R. Reddy, C.-L. Chen, Y.-H. Liu, S.-M. Peng, J.-T. Chen, S.-T. Liu, *Organometallics* **1999**, *18*, 2574−2576. − [12f] B. Crociani, S. Antonaroli, G. Bandoli, L. Canovese, F. Visentin, P. Uguagliati, *Organometallics* **1999**, *18*, 1137−1147.

[13] E. Mugnaini, P. Grünanger, *Atti. Accad. Naz. Lincei, Cl. Sci. Fis. Mat. Nat., Rend.* **1953**, *14*, 958.

[14] J. H. Satcher, Jr., M. W. Droege, T. J. R. Weakley, R. T. Taylor, *Inorg. Chem.* **1995**, *34*, 3317−3328.

[15] [15a] G. Aullon, D. Bellamy, L. Brammer, E. A. Bruton, A. G. Orpen, *Chem. Commun.* **1998**, 653−654. − [15b] C. B. Aakeröy, T. A. Evans, K. R. Seddon, I. Palinko, *New J. Chem.* **1999**, 145−152.

[16] D. B. Grotjahn, D. Combs, S. Van, G. Aguirre, F. Ortega, *Inorg. Chem.* **2000**, *39*, 2080−2086.

[17] D. Nicholls, in *Comprehensive Inorganic Chemistry* (Eds.: J. C. Bailar, H. J. Emeleus, Sir R. Nyholm, A. F. Trotman-Dickenson), 1st ed., Pergamon, Oxford, **1973**, vol. 3, p. 1152 ff.

[18] [18a] G. M. Sheldrick, *SHELXL-97, Program for Crystal Structure Refinement*, Universität Göttingen, **1997**. − [18b] G. M. Sheldrick, *SHELXS-97, Program for Crystal Structure Solution*, Universität Göttingen, **1997**.

Received March 7, 2001
[I01085]